Search for SUSY at LHC in the first year of data-taking.

Abstract

If Supersymmetry would manifest itself at a low mass scale it might be found already in the early phase of the LHC operation. Generic signatures for Supersymmetry in pp-collisions consist of high jet multiplicity, large missing transverse energy as well as leptons in the final state. The CMS search strategy and prospects for a SUSY discovery in the first year of data-taking is reviewed.

Michele Pioppi[1] *on behalf of the CMS collaboration*
Imperial College London
South Kensington Campus,
London SW7 2AZ, United Kingdom

1 Introduction

The Large Hadron Collider (LHC) [1] at CERN opens a new energy regime offering a very exciting discovery potential for physics beyond the Standard Model. In this paper the search for Supersymmetry (SUSY) in the startup scenario at $\sqrt{s} = 10$ TeV is discussed. Supersymmetry exists in many theories beyond the Standard Model. Two of the best studied braking mechanisms are the Minimal SuperGravity (mSUGRA) and Gauge Mediated Symmetry Breaking (GMSB). Benchmark points have been defined in the framework of mSUGRA and GMSB to study various experimental SUSY signatures. In the CMS experiment [2] SUSY analyses are organized according to topologies, e.g. number of leptons, photons and jets in the final state, which arise from SUSY cascades. A detailed definition of the benchmark points can be found here [3].

The paper is organized as follows: in Section 2 the SUSY search in multijet final state is discussed [4]. Searches for new physics in diphoton [5] and dilepton [6] final state are described in section 3 and 4 respectively.

2 Search for SUSY in fully hadronic final state

This section describes a search strategy for a possible discovery of SUSY signatures with the CMS detector at the LHC using exclusive n-jet events ($n = 2 \ldots 6$). The

[1] also with INFN Perugia, Italy

event topology under investigation consists of n high-p_{T} jets and two invisible neutralinos which lead to a missing energy signature. The high-p_{T} jets are produced in the decay chains of the initially produced heavy squarks and gluinos. The main aim of the analysis is to develop a robust measurement technique suitable for the early physics data at the LHC and stable with respect to jet energy mismeasurements. Before applying any event selection, multijet production from QCD is the dominant process, where missing energy is introduced through jet mismeasurements.

2.1 Trigger and selection

The benchmark points of mSUGRA LM0 and LM1 are used to estimate the trigger efficiency for signal events. Both signal points have 100% efficiency after all cuts for the single jet trigger HLT_Jet110 (one jet with corrected jet transverse momentum $>$ 110 GeV/c).

Hadronic jets are reconstructed from calorimeter energy deposits which are clustered using an iterative cone algorithm with $R = 0.5$ [7]. Furthermore, these jets are required to have a transverse momentum greater than 50 GeV/c, pseudo-rapidity $|\eta| < 3.0$, and an electromagnetic fraction $F_{\mathrm{em}} < 0.9$. The transverse momentum of the leading jet and second leading jet need to exceed 100 GeV/c and the pseudo-rapidity of the leading jet is required to be smaller than two. Based on the jets defined above two additional variables are defined: H_{T} as the scalar sum over the transverse momenta of the selected jets in an event, $H_{\mathrm{T}} = \sum_i p_{\mathrm{T}}^{j_i}$ and the missing transverse momentum of the event calculated as $\vec{H}_{\mathrm{T}}^{\mathrm{miss}} = -\sum_i \vec{p_{\mathrm{T}}}^{j_i}$. In order to reduce background events from SM processes H_{T} is required to be greater than 350 GeV/c.
All events are rejected where either an isolated muon [8] with $p_{\mathrm{T}} > 10$ GeV/c or an isolated electron [9] with $p_{\mathrm{T}} > 10$ GeV/c or photons [3] with $p_{\mathrm{T}} > 25$ GeV/c or jets with $p_{\mathrm{T}} > 50$ GeV/c that does not fulfill the other criteria ($|\eta| < 3$ or $F_{\mathrm{em}} < 0.9$) are found.

2.2 Analysis method and results

In the following a kinematic variable (α_{T}) is used that allows separation of signal events with real missing energy from QCD events in which missing energy is created by jet energy mismeasurements.
In the dijet case ($n = 2$) transverse momentum conservation requires the p_{T} of the two jets in QCD events to be of equal magnitude and back-to-back in the azimuthal angle ϕ. The variable α_{T}, first introduced in Ref. [10], exploits exactly this requirement. It is defined as

$$\alpha_{\mathrm{T}} = E_{\mathrm{T}}^{j2}/\mathrm{M}_{\mathrm{T}} \tag{1}$$

	$\mathrm{QCD}_{\mathrm{MadGraph}}$	$\mathrm{Z} \to \nu\overline{\nu}$	$\mathrm{W} \to \nu\ell$	$\mathrm{t\bar{t}}$	$\mathrm{Z} \to \ell\ell$	LM1	LM0
dijet	0.0+1.0	2.8±0.7	5.0±1.4	0.3±0.1	0.0+0.3	52±1	68±3
$n_j > 2$	$0.9^{+1.0}_{-0.9}$	10.0±1.4	10.4±1.7	8.8±0.8	$0.3^{+0.4}_{-0.3}$	116±1	253±6

Table 1: Numbers of events expected for the dijet case and for $n = 3 \ldots 6$ jets case for background samples (QCD, $\mathrm{Z} \to \nu\overline{\nu}$+jets, W+jets, $\mathrm{t\bar{t}}$ and Z+jets) and the LM0 and LM1 signal points. The final numbers of selected events are shown after the cuts on α_{T} and $R(H_{\mathrm{T}}^{\mathrm{miss}})$.

where E_{T}^{j2} is the transverse energy of the second leading jet in the event and $\mathrm{M_T}$ is defined as

$$\mathrm{M_T} = \sqrt{\left(\sum_{i=1}^{n} E_{\mathrm{T}}^{j_i}\right)^2 - \left(\sum_{i=1}^{n} p_x^{j_i}\right)^2 - \left(\sum_{i=1}^{n} p_y^{j_i}\right)^2} = \sqrt{H_{\mathrm{T}}^2 - (H_{\mathrm{T}}^{\mathrm{miss}})^2} \quad , \qquad (2)$$

and $n = 2$ in the dijet case. For a well measured QCD dijet event, $E_{\mathrm{T}}^{j2} = 0.5 \times H_T$ and $H_{\mathrm{T}}^{\mathrm{miss}} = 0$, thus α_{T} is exactly 0.5.

To define α_{T} for more than two jets the n-jet system is reduced down to a two-jet system by combining jets into two pseudo-jets. The E_{T} of the pseudo-jets is calculated as the scalar sum of the contributing jet E_{T}. All possibilities of how n jets can be combined into two are tested and the combination is chosen where the resulting pseudo-jet E_{T} are most similar, *i.e.*, for which the difference $\Delta H_{\mathrm{T}} = E_{\mathrm{T}}^{pj_1} - E_{\mathrm{T}}^{pj_2}$ is minimal. For n jets, α_{T} is then obtained in the same way as in Eq. 1.

In the event selection H_{T} is required to be greater than 350 GeV/c which is well above the transverse momentum threshold of 50 GeV/c for a single jet. However several jets below that threshold could still lead to a considerable amount of ignored momentum in the event. For that reason the $H_{\mathrm{T}}^{\mathrm{miss}}$ determined using all jets having a p_{T} larger than 30 GeV/c , $H_{\mathrm{T}}^{\mathrm{miss}}(\mathrm{jet}\, p_{\mathrm{T}} > 30$ GeV/c), is calculated and compared to the $H_{\mathrm{T}}^{\mathrm{miss}}$ determined from the selected jets only, $H_{\mathrm{T}}^{\mathrm{miss}}$(selected jets). The ratio

$$R(H_{\mathrm{T}}^{\mathrm{miss}}) = H_{\mathrm{T}}^{\mathrm{miss}}(\text{selected jets}) / H_{\mathrm{T}}^{\mathrm{miss}}(\mathrm{jet}\, p_{\mathrm{T}} > 30 \text{ GeV/c}) \qquad (3)$$

can be used to single out events where the inclusion of lower momentum jets does significantly improve the balance of the event. If the missing transverse energy ($H_{\mathrm{T}}^{\mathrm{miss}}$) is increased by 25% due to the fact that the transverse momentum threshold of the selected jets is 50 GeV/c and not 30 GeV/c the event is rejected, thus $R(H_{\mathrm{T}}^{\mathrm{miss}})$ is required to be smaller than 1.25.

The α_{T} distributions for the dijet case and the sum of $n = 3 \ldots 6$ jets case are shown in Fig. 1 where the requirement on $R(H_{\mathrm{T}}^{\mathrm{miss}})$ has already been applied. In both figures the QCD background peaks, as expected, sharply at a value of 0.5. To

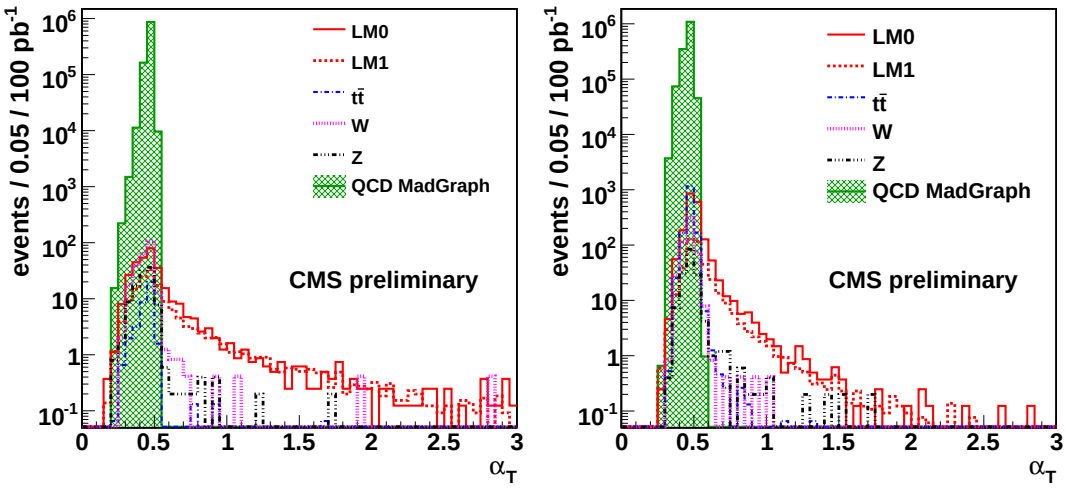

(a) Distribution of α_T for dijet events.

(b) Distribution of α_T for events with $n = 3 \ldots 6$ jets.

Figure 1: α_T distribution.

account for finite jet energy and ϕ resolutions events are only selected if α_T is larger than 0.55.

The resulting event yields for signal and background are summarized in Tab. 1. All expected event yields correspond to an integrated luminosity of $100\,\mathrm{pb}^{-1}$. It can be seen that in the dijet case only $\mathrm{Z} \to \nu\overline{\nu}$ + jets and W + jets events give a small background contribution over a clear signal. At higher jet multiplicities $n = 3 \ldots 6$, top decays as well as about one QCD event contribute to the remaining background after the final selection.

2.3 Establishing a Signal incompatible with Standard Model Background in Data

To establish the discovery of a SUSY signal the fact that signal events are produced more centrally in pseudo-rapidity compared to the SM backgrounds, in particular compared to QCD events whose main production mechanism is t-channel exchange, is used. The pseudo-rapidity of the leading jet can be used as a measure of the centrality of an event. For the SM background the ratio $R_{\alpha_\mathrm{T}}(0.55)$ of events with α_T larger than the cut value over that of events with α_T smaller than the cut value, is, as shown in Fig. 2(a), approximately constant as a function of pseudo-rapidity and independent of H_T. $R_{\alpha_\mathrm{T}}(0.55)$ behaves very differently in the presence of a SUSY

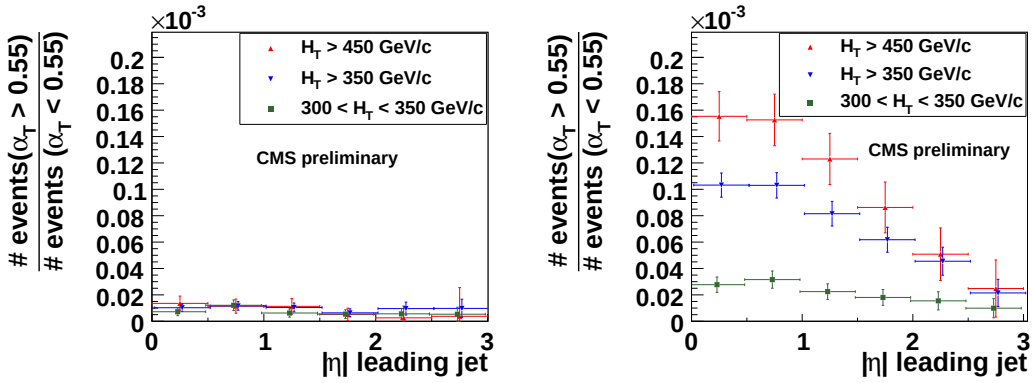

(a) SM background only

(b) SUSY(LM0) + SM background

Figure 2: $R_{\alpha_T}(0.55)$ as a function of $|\eta|$ for different H_T cuts for SM background only and in case of presence of a SUSY signal. The error bars indicate the expected statistical uncertainties for a data sample of 100 pb^{-1}.

signal as illustrated in Fig. 2(b) for the LM0 benchmark point. As can be seen, the presence of a SUSY signal manifests itself with two distinct features: $R_{\alpha_T}(0.55)$ exhibits a negative slope with larger values of $|\eta|$; tighter requirements on H_T result in a steeper slope and an offset in $R_{\alpha_T}(0.55)$. For events with $H_T > 350$ GeV/c the measured $R_{\alpha_T}(0.55)$ in the central $|\eta|$ bins is well above the ratios obtained from the control region $300 < H_T < 350$ GeV/c and increases with smaller values of η. Even with a systematic uncertainty of 100% on $R_{\alpha_T}(0.55)$ in the control region the excess would remain convincing.

3 Search for SUSY in diphoton final state

The final state with two high E_T photons and large missing transverse energy can harbor new physics signals in a variety of theoretical scenarios, most notably GMSB. In this section, a data-driven strategy that can be used in a plausible start-up scenario to predict the E_T^{miss} distribution in a diphoton sample from the SM processes is described. Observation of an excess of events at high E_T^{miss} would be a signature of new physics.

The SM contribution to diphoton plus E_T^{miss} final state is small. The only physics backgrounds are $Z\gamma\gamma \to \nu\nu\gamma\gamma$ and $W\gamma\gamma \to \ell\nu\gamma\gamma$. The instrumental background has three major components. The first component results from QCD events with no true E_T^{miss} (QCD background), such as direct diphoton, photon plus jets, and multijet

production. The second component comes from events with real $E_{\mathrm{T}}^{\mathrm{miss}}$ (Electroweak background). This component is dominated by $W\gamma$ and Wj production where the W decays into an electron plus a neutrino when the electron is mis-reconstructed as a photon. The third background is associated with the high energy muons from cosmic rays or beam halo (Non-beam background).

3.1 Trigger and selection

The trigger applied in this analysis requires a photon with E_{T} >25 GeV. This trigger is expected to run unprescaled for the duration of the first CMS run, and is fully efficient for the SUSY signal considered.

For the photon candidate selection, two objects in the ECAL Barrel ($|\eta| \leq 1.45$) with p_{T} >30 GeV/c were required to be isolated and to have a negligible deposit of energy in the hadronic calorimeter around the photon. The selected objects are classified as electrons if they have an associated track stub in the pixel detector, referred to as pixel seed, and as photons otherwise. In this way three independent samples are defined: $\gamma\gamma$ sample comprising events with at east two photons; $e\gamma$ sample with at least one electron and at least one photon; ee sample with at least two electrons.

Finally a cut $E_{\mathrm{T}}^{\mathrm{miss}} > 80$ GeV is applied to reduce significantly the SM background. The results of the selection are reported in Tab. 2

	$\gamma\gamma$	γ+jet	multijets	W, W+nγ	Z, Z+nγ	GM1c
all events	1055 ± 4	3189 ± 100	173 ± 37	8.5 ± 3.0	23± 1.3	20.7
after $E_{\mathrm{T}}^{\mathrm{miss}}$	1.3 ± 0.16	1.3 ± 0.16		0.09± 0.04	0.09± 0.02	14.8

Table 2: Event counts before and after the cut on $E_{\mathrm{T}}^{\mathrm{miss}}$ for the $\gamma\gamma$ sample for 100 pb^{-1} at 10 TeV.

3.2 Non-beam background

Energetic cosmic muons or muons from beam halo can emit photons as they pass through the ECAL. The shower shape and arrival time of these photons is slightly different from the ones originating from the interaction point, especially for beam halo.

Photons from the interaction point hit a crystal approximately perpendicular to the face because the crystals are rotated in η such that they point back to the interaction point. As a result of this rotation, photons from the interaction point give rise to showers with a small spread in η. However, photons from the beam halo

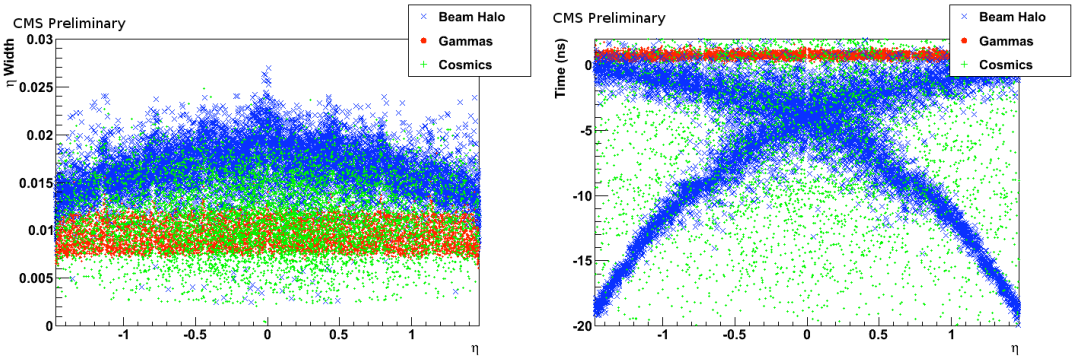

(a) Photon shower width along η versus photon η

(b) Measured cluster time versus η

Figure 3: Photon shower and Timing in beam halo, cosmics, and photon gun events.

traveling parallel to the beam tend to have a large spread in η. Cosmic ray photons come from all possible angles and could have very narrow or very wide showers. Fig. 3(a) displays the distribution of the energy-weighted RMS of the shower profile in η (η-width) for the three sources of photons.

The expected time resolution for individual crystals is better then 1 ns, and the non-beam backgrounds can be discriminated against using the measured cluster time. Cosmic background is asynchronous, but beam halo has a very specific time distribution. Protons and halo muons travel parallel to each other and have the same $z(t)$. The time difference between the photons from the IP and halo is then given by $\Delta t = (Z + \sqrt{Z^2 + R^2})/c$. The value of R, the radius of the shower in the ECAL, is not known. Fortunately, the resulting uncertainty in Δt is fairly small, as shown in Fig. 3(b), which shows the comparison of the measured time of the photons from beam halo, cosmics, and prompt photons, corrected for the detector geometry.

Although the exact amount of non-beam backgrounds is very hard to predict, a combination of the two techniques explored above (shower shape and timing) will be sufficient for the effective elimination of these backgrounds. It will also be possible to isolate a pure sample of non-beam backgrounds, ensuring a reliable estimation of the residual contamination.

3.3 Determination of $E_{\mathrm{T}}^{\mathrm{miss}}$ Distribution from Data

The contribution of the Electroweak background is determined using the $e\gamma$ sample. The $E_{\mathrm{T}}^{\mathrm{miss}}$ distribution in $e\gamma$ sample is multiplied by $f_{e\to\gamma}/(1 - f_{e\to\gamma})$, where $f_{e\to\gamma}$ is the electron-photon mis-identification rate. $f_{e\to\gamma}$ is obtained by fitting the mass

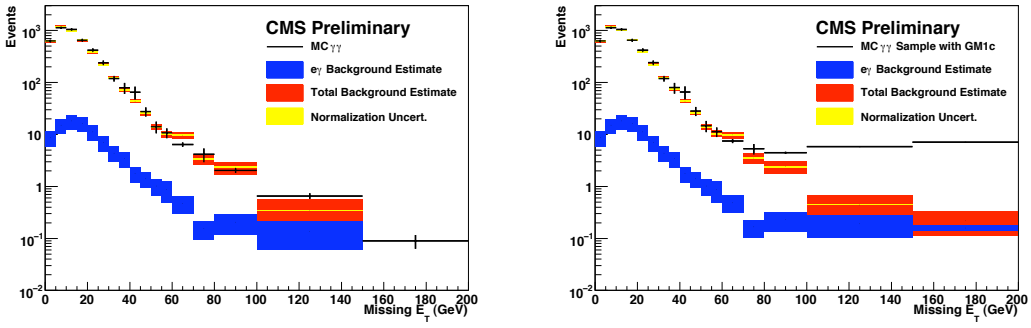

(a) SM background only

(b) SUSY(GM1c) + SM background

Figure 4: Background closure test using $Z \rightarrow e^+e^-$ events to describe the QCD background.

of the Z for the ee sample and $e\gamma$ sample, and by comparing the integrals of these fits. The resultant distribution is taken as an estimate of the this background and is subtracted prior to assessing the background from QCD events.
The $E_{\mathrm{T}}^{\mathrm{miss}}$ distribution for the QCD background is modelled using a sample of Z$\rightarrow ee$ events, selected from ee sample with invariant mass cut on the two electrons, $80 < M_{ee} < 100$ GeV.

The key assumption is that the di-EM system which is measured comparitively well, and the recoil and other hadronic activity which is measured poorly can be separated in the event. The di-EM p_T is used as a measure of this additional activity. Its amount is different for the Z$\rightarrow ee$ and the $\gamma\gamma$ events. To obtain the proper shape of the $E_{\mathrm{T}}^{\mathrm{miss}}$ distribution, the Z$\rightarrow ee$ events are reweighted so that their di-EM p_T distribution matches the one in the $\gamma\gamma$ sample. The weighted $E_{\mathrm{T}}^{\mathrm{miss}}$ distribution is then normalized to the $\gamma\gamma$ sample in the low missing transverse energy ($E_{\mathrm{T}}^{\mathrm{miss}} < 20$ GeV) region.

Fig. 4(a) show the closure test for $Z \rightarrow e^+e^-$ sample used for QCD background determination in absence of SUSY signal. The presence of the signal can bias the background estimation, thus the entire analysis is repeated with GM1c SUSY signal mixed in, as shown in Fig. 4(b).

The data driven estimation of the background agrees very well with the number of expected events evaluated with the MC truth, as shown in Tab. 3.

	MC truth			Data-driven	
	$N_{\gamma\gamma}^{QCD}$	$N_{\gamma\gamma}^{EWK}$	N^{GM1c}	N_{BG}^{QCD}	N_{BG}^{EWK}
no SUSY	2.61 ± 0.23	0.17 ± 0.04		2.34 ± 0.65	0.35 ± 0.10
with SUSY	2.61 ± 0.23	0.17 ± 0.04	14.8 ± 0.1	2.48 ± 0.67	0.50 ± 0.10

Table 3: Closure test for $\gamma\gamma$ sample with and without GM1c SUSY signal. The number of events corresponds to 100 pb^{-1} at 10 TeV.

4 SUSY discovery potential and measurement of a dilepton mass edge

In mSUGRA models the lightest neutralino escapes detection and no mass peaks can be observed in SUSY decay chains. Of special interest are robust signatures such as edges in mass distributions in leptonic final states which can be probed with the CMS experiment.

The purpose of this analysis is to observe a significant excess of opposite sign same flavour leptons over the various backgrounds and to measure the endpoint in the invariant mass distribution. All flavour symmetric background (including SUSY decays of this type) can be determined from data events with opposite sign opposite flavour leptons. The aim is to perform such an analysis already with the first LHC data which is expected to amount to roughly 200-300 pb^{-1} in 2010.

The leptonic decay of the next-to-lightest neutralino gives a characteristic signature. This decay can proceed in different ways even in the mSUGRA model. A mass difference of the neutralinos smaller than the Z boson mass and any slepton mass leads to a three body decay. In that case the endpoint in the lepton invariant mass represents directly the mass difference of the two lightest neutralinos

$$m_{ll,max} = m_{\tilde{\chi}_2^0} - m_{\tilde{\chi}_1^0} \tag{4}$$

A two-body decay occurs via a real slepton and is allowed if at least one slepton is lighter than the mass difference of the neutralinos. In that case the endpoint can be expressed by

$$(m_{ll}^{max})^2 = \frac{\left(m_{\tilde{\chi}_2^0}^2 - m_{\tilde{l}}^2\right)\left(m_{\tilde{l}}^2 - m_{\tilde{\chi}_1^0}^2\right)}{m_{\tilde{l}}^2} \tag{5}$$

where $m_{\tilde{l}}$ is the mass of the intermediate slepton. The shape of the mass edge results only from kinematics and is triangular.

4.1 Trigger and selection

Single lepton (electron or muon) trigger is used in this analysis. Since the leptons originating from the signal decay have a very soft p_{T} spectrum, the triggers with the lowest available threshold for electrons ($p_{\mathrm{T}} > 15$ GeV/c) and muons ($p_{\mathrm{T}} > 11$ GeV/c) are used.

The base selection requires two isolated leptons of opposite sign. Muon identification requires reconstruction in both the muon system and the inner tracker [8]. Each electron has to fulfill the tight electron identification criteria, which consist of a set of cuts depending on the electron p_{T} and η [9]. Additionally a $p_{\mathrm{T}} > 10$ GeV/c and $|\eta| < 2$ is required for each lepton. To stay above the trigger threshold the first lepton is required to have a $p_{\mathrm{T}} > 16$ GeV/c. The main SUSY selection is based on jets and missing transverse energy. The cuts have not been optimized at a certain benchmark point, but should reflect the general SUSY signature. The selection requires three jets with $p_{\mathrm{T}}^{\mathrm{j1}} > 100$ GeV/c, $p_{\mathrm{T}}^{\mathrm{j2}} > 50$ GeV/c, and $p_{\mathrm{T}}^{\mathrm{j3}} > 50$ GeV/c. A missing transverse energy of at least 100 GeV is required.

Sample	tt+jets	Z+jets	W+jets	Diboson	Dijet	LM0 signal	LM0 incl.
N_{events}	80	1	2	0	0	87	362

Table 4: Number of selected events using the described event selection for an integrated luminosity of 200 pb^{-1}.

The number of events obtained after the selection is listed in Tab. 4. All background which leads to uncorrelated lepton pairs can be measured directly from data [11]. In order to extrapolate to the same flavour opposite sign lepton pair distribution the opposite sign opposite flavour lepton pairs and use this distribution are selected. With this method one is able to predict all backgrounds which produce uncorrelated leptons such as W, $t\bar{t}$, dijet and WW events.

The invariant mass distribution of all opposite sign same flavour leptons for $200\,\mathrm{pb}^{-1}$ is shown in Fig. 5(a). The opposite sign opposite flavour distribution used to extrapolate the background is displayed in Fig. 5(b).

4.2 Determination of the mass edge

The model used for the fit of the mass edge consists of three parts. To model the signal the theoretical model [12, 13] convoluted numerically with a gaussian has been

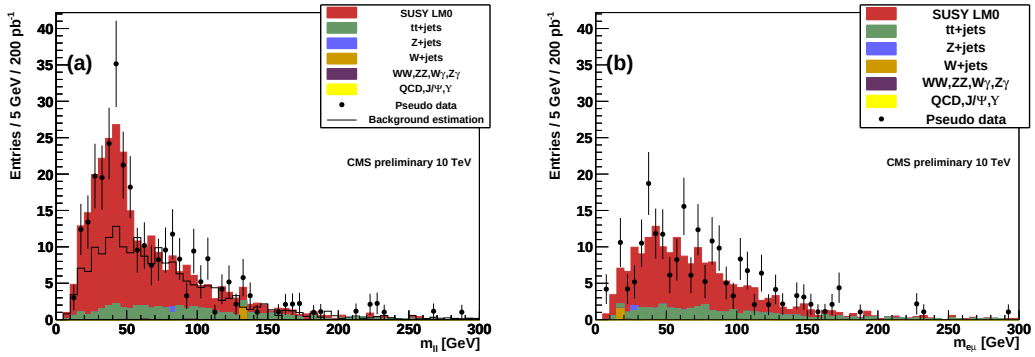

(a) ee, $\mu\mu$ (b) $e\mu$

Figure 5: DiLepton invariant mass. The black solid line represents the extrapolation from the opposite flavour distribution. The black points represent pseudo data of one experiment where no scaling has been applied but exactly 200 pb^{-1} of MC events have been analysed.

used in case of a 3-body decay

$$S(m_{ll}) = \frac{1}{\sqrt{2\pi}\sigma} \int_0^{m_{cut}} dy \cdot y \frac{\sqrt{y^4 - y^2\left(m^2 + M^2\right) + \left(m\,M\right)^2}}{\left(y^2 - m_Z^2\right)^2} \times \left(-2y^4 - y^2\left(m^2 + 2M^2\right) + \left(m\,M\right)^2\right) e^{\frac{-(m_{ll}-y)^2}{2\sigma^2}} \tag{6}$$

where $m = m_{\tilde{\chi}_2^0} - m_{\tilde{\chi}_1^0}$ is the difference, $M = m_{\tilde{\chi}_2^0} + m_{\tilde{\chi}_1^0}$ is the sum in neutralino mass and M_Z is the Z mass, which is kept fixed. In case of the two-body decay the signal model consists of a triangle convoluted with a gaussian

$$T(m_{ll}) = \frac{1}{\sqrt{2\pi}\sigma} \int_0^{m_{cut}} dy \cdot y e^{\frac{-(m_{ll}-y)^2}{2\sigma^2}} \tag{7}$$

A curve parametrized as

$$B(m_{ll}) = m_{ll}^a \cdot e^{-b \cdot m_{ll}} \tag{8}$$

has been used to fit the opposite sign opposite flavour invariant mass distribution. Additionally the Z peak is fitted using a Breit-Wigner convoluted with a gaussian. The number of signal N_{Sig}, background N_{Bkg} and Z events N_Z are fitted as well.

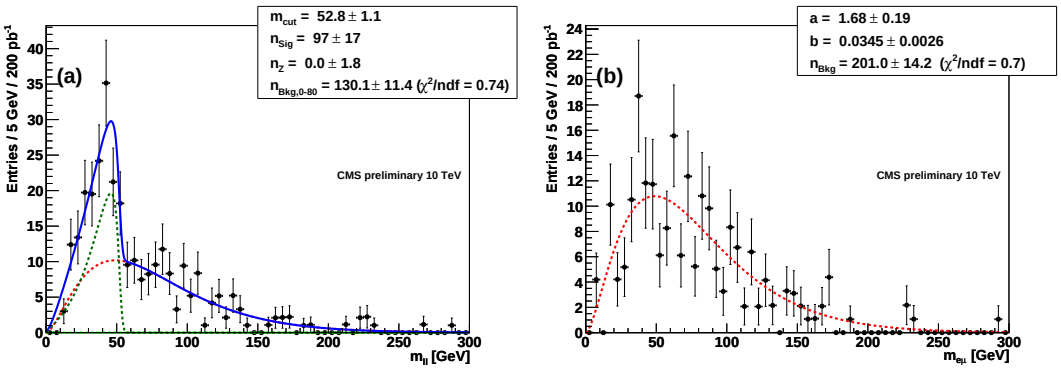

(a) ee, $\mu\mu$ invariant mass distributions

(b) $e\mu$ invariant mass distribution

Figure 6: The combined fit at LM0, the green curve represents the SUSY signal model, the red curve is the background function and the light green dashed line the Z contribution.

4.3 Expected results

A simultaneous fit to the the ee, $\mu\mu$ (signal plus background model) and $e\mu$ (background model) invariant mass distributions is performed.

The fit to the invariant mass distributions at LM0 is shown in Fig. 6(a) and it yields a value of $m_{ll,max} = (52.8 \pm 1.1)$ GeV for the dataset of exactly 200 pb^{-1} and $m_{ll,max} = (51.3 \pm 1.5)$ GeV for the full MC data where the error is the one expected after 200 pb^{-1}. The derived number of signal events $n_{sig} = 97 \pm 17$ agrees with the number of signal events from MC truth (Tab. 4). The theoretical endpoint $m_{ll,theo} = 52.7$ GeV is reproduced in case of the fit with the three-body decay model. The background fit of the opposite sign opposite flavour lepton pairs is shown in Fig. 6(b). The total number of background events is $n_{Bkg} = 201 \pm 14$ which is in agreement with the expected number from MC truth (192).

The main sources of systematic uncertainties are the jet energy scale, the electron energy scale, the lepton efficiency and the modeling of the background and of the resolution. Combining systematic and statistical errors, the expected results for LM0 and 200 pb^{-1} at 10 TeV is

$$m_{ll,max} = (51.3 \pm 1.5_{stat.} \pm 0.9_{syst.}) \text{ GeV/c} \tag{9}$$

compared to a theoretical value of 52.7 GeV.

5 Summary

The strategy for three different analyses aimed to discovery SUSY in the first year of data-taking at LHC considering $\sqrt{s} = 10\,\text{TeV}$ with the CMS experiment were presented.

The search for SUSY in multijet final state is carried out in the context of SUSY for several sets of parameters in the mSUGRA parameter space assuming an integrated luminosity of 100 pb^{-1}. The discrimination power of α_{T} against SM background from QCD events provides, for favourable SUSY benchmark points, signal over background ratios of 4 to 8 depending on the considered jet multiplicity bin.

In the context of the GMSB models a strategy to infer the existence of new physics in diphoton events with large missing transverse energy has been developed. Background contribution in the high $E_{\text{T}}^{\text{miss}}$ region is estimated can be precisely estimated with a pure data-driven method in 100 pb^{-1}.

A significant excess of SUSY opposite sign same flavour lepton pairs can be found within the first 200 pb^{-1} at LM0. The signal provides a quite robust signature and the background determination directly from data is possible. At LM0 the combined fit of the dileptonic endpoint is possible with 200 pb^{-1} with an expected uncertainty of 1.8 GeV.

References

[1] **JINST 3 (2008) S08004**, L. Evans, P.Bryant, *"LHC machine"*

[2] **JINST 3 (2008) S08004**, The CMS coll., *"The CMS experiment at the CERN LHC"*

[3] **J. Phys. G: Nucl. Part. Phys. 34** (2007), The CMS coll., *"CMS Physics Technical Design Report, Volume II: Physics Performance"*

[4] **PAS SUS-09-001**, The CMS coll., *"Search strategy for exclusive multijet events from Supersymmetry"*

[5] **PAS SUS-09-004**, The CMS coll., *"Data-Driven Background Estimates for SUSY diphoton Searches"*

[6] **PAS SUS-09-002**, The CMS coll., *"Discovery potential and measurement of a dilepton mass edge in SUSY events at sqrt(s) = 10 TeV"*

[7] **PAS JME-07-003**, The CMS coll., *"Performance of Jet Algorithms in CMS"*

[8] **CMS-NOTE 2006/010**, The CMS coll., *"Muon Identification in CMS"*

[9] **CMS-NOTE 2006/040**, The CMS coll., *"Electron Reconstruction in CMS"*

[10] **PAS SUS-08-005**, The CMS coll., *"SUSY Searches with dijet Events"*

[11] **PAS SUS-08-001**, The CMS coll., *"Dilepton + Jets + MET channel : Observation and Measurement of* $\tilde{\chi}_2^o \to \tilde{\chi}_1^o \ell\ell$*"*

[12] **Phys.Rev.D 60** (1999), M. M. Nojiri and Y. Yamada, *"Neutralino decays at the CERN LHC"*

[13] **Eur.Phys.J.C 52** (2007), U. de Sanctis et al., *"Perspectives for the detection and measurement of Supersymmetry in the focus point region of mSUGRA models with the ATLAS detector at LHC"*